Johann Radon Institute for
Computational and Applied Mathematics
Austrian Academy of Sciences (ÖAW)

Coupling fluid-structure interaction with phase-field fracture: modeling and a numerical example

T. Wick

RICAM-Report 2015-22

Coupling fluid-structure interaction with phase-field fracture: modeling and a numerical example

Thomas Wick[1]

RICAM, Austrian Academy of Sciences, Altenberger Str. 69,
4040 Linz, Austria
thomas.wick@ricam.oeaw.ac.at

Abstract. In this work, a framework for coupling arbitrary Lagrangian-Eulerian fluid-structure interaction with phase-field fracture is suggested. The key idea is based on applying the weak form of phase-field fracture, including a crack irreversibility constraint, to the nonlinear coupled system of Navier-Stokes and elasticity. The resulting setting is formulated via variational-monolithic coupling and has four unknowns: velocities, displacements, pressure, and a phase-field variable. The inequality constraint is imposed through penalization using an augmented Lagrangian algorithm. The nonlinear problem is solved with Newton's method. The framework is tested in terms of a numerical example in which computational stability is demonstrated by evaluating goal functionals on different spatial meshes.

1 Introduction

Both fluid-structure interaction (FSI) and fracture propagation are current but challenging topics with numerous applications in applied mathematics and engineering. In this work, we want to bring both frameworks together. The idea is to employ the nowadays standard arbitrary Lagrangian-Eulerian (ALE) technique [12,7] for coupling the isothermal, incompressible Navier-Stokes equations with the geometrically nonlinear Saint Venant Kirchhoff model. The resulting formulation using variational-monolithic coupling is outlined in [11,20]. Here, three unknowns are sought: velocities, pressure and displacements. On the other hand, brittle fracture propagation using variational techniques has attracted attention since the pioneering work in [8]. We specifically follow the phase-field fracture methodology from [14] that has been extended to pressurized fractures in [17,16]. Here, the crack irreversibility constraint has been imposed through penalization. In phase-field fracture, two unknowns are sought: displacements and a phase-field function that determines the crack location. A first (minor) novelty of this paper is an augmented Lagrangian penalization for a fully-coupled phase-field fracture framework. This is in contrast to [19] in which the displacement phase-field system has been solved in a partitioned fashion. Such a technique has been employed due to the fact that the underlying energy functional is non-convex in both variables simultaneously [4,3], which causes serious challenges in the

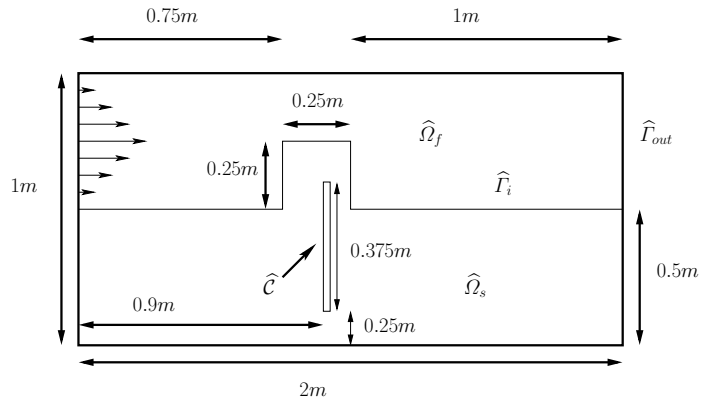

Fig. 1. Configuration and notation.

numerical solution. Recently, a robust (but heuristic) methodology of a quasi fully-coupled approach has been proposed in [9] where the phase-field variable has been time-lagged in the displacement equation.

Since the solid part of FSI is based on elastodynamics, we accentuate the work of [2,13,5] who extended variational quasi-static brittle fracture to dynamic brittle fracture taking into account the solid acceleration term. Collecting all these different pieces allows us to apply the phase-field fracture technique to the solid part of the FSI problem. More specifically, the phase-field part is re-written (similarly to the flow problem in FSI) in ALE coordinates. The resulting formulation is consequently prescribed in a fixed, but arbitrary, reference domain and all coupling conditions are satisfied in a variational exact fashion on the continuous level. The numerical discretization is then straightforward as the Rothe method (first time, then space) can be applied on the resulting semilinear form. The nonlinear coupled problem is solved with Newton's method. The outline of this paper is as follows: In Section 2, the equations are gathered; followed by brief hints in Section 3 on the discretization and numerical solution. The framework is tested in Section 4 with a prototype example in which computational stability for certain goal functional values is shown.

2 Notation, Spaces, Equations

We denote by $\Omega := \Omega(t) \subset \mathbb{R}^d$, $d = 2$, the domain of the FSI phase-field fracture problem; see Figure 1. This domain consists of three time-dependent subdomains $\Omega_f(t), \Omega_s(t)$ and $\mathcal{C}(t)$. We assume $\mathcal{C}(t) \subset\subset \Omega_s(t)$. The FSI-interface between $\Omega_f(t)$ and $\Omega_s(t)$ is denoted by $\Gamma_i(t) = \partial\Omega_f(t) \cap \partial\Omega_s(t)$. The initial (or later reference) domains are denoted by $\widehat{\Omega}, \widehat{\Omega}_f$ and $\widehat{\Omega}_s$, respectively, with the interface $\widehat{\Gamma}_i = \partial\widehat{\Omega}_f \cap \partial\widehat{\Omega}_s$. Furthermore, we denote the outer boundary

by $\partial\widehat{\Omega} = \widehat{\Gamma} = \widehat{\Gamma}_D \cup \widehat{\Gamma}_{out}$ where $\widehat{\Gamma}_D$ and $\widehat{\Gamma}_{out}$ denote Dirichlet and outflow Neumann boundaries, respectively. Specifically, $\widehat{\Gamma}_{out}$ is motivated by [10]. We denote the L^2 scalar product with $(\cdot,\cdot)$ as frequently used in the literature. Finally, let T the end time value. For the function spaces, we set:

$$\begin{aligned}
\hat{L}_f &:= L^2(\widehat{\Omega}_f), \quad \hat{L}_s := L^2(\widehat{\Omega}_s), \quad \hat{L}_f^0 := L^2(\widehat{\Omega}_f)/\mathbb{R}, \quad \hat{L}_s^0 := L^2(\widehat{\Omega}_s)/\mathbb{R},\\
\hat{V}_f^0 &:= H_0^1(\widehat{\Omega}_f), \quad \hat{V}_{f,\hat{v}}^0 := \{\hat{v}_f \in H_0^1(\widehat{\Omega}_f) : \hat{v}_f = \hat{v}_s \text{ on } \widehat{\Gamma}_i\},\\
\hat{V}_s^0 &:= H_0^1(\widehat{\Omega}_s), \quad \hat{V}_{f,\hat{u}}^0 := \{\hat{u}_f \in H_0^1(\widehat{\Omega}_f) : \hat{u}_f = \hat{u}_s \text{ on } \widehat{\Gamma}_i\},\\
\hat{V}_{f,\hat{u},\widehat{\Gamma}_i}^0 &:= \{\hat{\psi}_f \in H_0^1(\widehat{\Omega}_f) : \hat{\psi}_f = \hat{\psi}_s \text{ on } \widehat{\Gamma}_i \subset \partial X\},\\
W &:= \{\varphi \in H^1(\Omega_s \cup \mathcal{C}) : \partial_t\varphi \leq 0 \text{ a.e. on } \Omega_s \cup \mathcal{C}\}.
\end{aligned}$$

2.1 Variational-monolithic ALE fluid-structure interaction

First, we define the ALE transformation:

Definition 1. The ALE mapping is defined in terms of the vector-valued fluid mesh displacement $\hat{u}_f$ (obtained by solving a mesh motion problem) such that

$$\hat{\mathcal{A}}(\hat{x},t) : \widehat{\Omega}_f \times I \to \Omega_f, \quad \text{with } \hat{\mathcal{A}}(\hat{x},t) = \hat{x} + \hat{u}_f(\hat{x},t), \tag{1}$$

which is specified through the deformation gradient and its determinant

$$\widehat{F} := \widehat{\nabla}\hat{\mathcal{A}} = \hat{I} + \widehat{\nabla}\hat{u}_f, \quad \hat{J} := \det(\widehat{F}). \tag{2}$$

Here, $\hat{I}$ denotes the identity matrix. The mesh velocity is defined by $\hat{w} := \partial_t\hat{\mathcal{A}}$ and is numerically realized as $\hat{w} = k^{-1}(\hat{u}_f - \hat{u}_f^{n-1})$, where $\hat{u}_f$ is the current displacement solution and $\hat{u}_f^{n-1}$ the previous time step solution, and $k := t^n - t^{n-1}$ being the time step size. The key quantity to measure the fluid mesh regularity is $\hat{J}$.

The weak form of a variational-monolithic FSI model reads, e.g., [20]:

Proposition 2. *Find vector-valued velocities, vector-valued displacements and a scalar-valued fluid pressure, i.e.,* $\{\hat{v}_f, \hat{v}_s, \hat{u}_f, \hat{u}_s, \hat{p}_f\} \in \{\hat{v}_f^D + \hat{V}_{f,\hat{v}}^0\} \times \hat{L}_s \times \{\hat{u}_f^D + \hat{V}_{f,\hat{u}}^0\} \times \{\hat{u}_s^D + \hat{V}_s^0\} \times \hat{L}_f^0$, *such that* $\hat{v}_f(0) = \hat{v}_f^0$, $\hat{v}_s(0) = \hat{v}_s^0$, $\hat{u}_f(0) = \hat{u}_f^0$, *and* $\hat{u}_s(0) = \hat{u}_s^0$ *are satisfied, and for almost all time steps holds:*

$$\begin{cases}
(\hat{J}\hat{\rho}_f\partial_t\hat{v}_f, \hat{\psi}^v)_{\widehat{\Omega}_f} + (\hat{\rho}_f\hat{J}(\widehat{F}^{-1}(\hat{v}_f - \hat{w})\cdot\widehat{\nabla})\hat{v}_f), \hat{\psi}^v)_{\widehat{\Omega}_f} + (\hat{J}\widehat{\sigma}_f\widehat{F}^{-T}, \widehat{\nabla}\hat{\psi}^v)_{\widehat{\Omega}_f}\\
+\langle\hat{\rho}_f\nu_f\hat{J}(\widehat{F}^{-T}\widehat{\nabla}\hat{v}_f^T\hat{n}_f)\widehat{F}^{-T}, \hat{\psi}^v\rangle_{\widehat{\Gamma}_{out}} = 0 \quad \forall\hat{\psi}^v \in \hat{V}_{f,\widehat{\Gamma}_i}^0,
\end{cases}$$

$$\left\{(\hat{\rho}_s\partial_t\hat{v}_s, \hat{\psi}^v)_{\widehat{\Omega}_s} + (\widehat{F}\widehat{\Sigma}, \widehat{\nabla}\hat{\psi}^v)_{\widehat{\Omega}_s} \quad = 0 \quad \forall\hat{\psi}^v \in \hat{V}_s^0,\right.$$

$$\left\{(\widehat{\sigma}_{mesh}, \widehat{\nabla}\hat{\psi}^u)_{\widehat{\Omega}_f} \quad = 0 \quad \forall\hat{\psi}^u \in \hat{V}_{f,\hat{u},\widehat{\Gamma}_i}^0,\right.$$

$$\left\{\hat{\rho}_s(\partial_t\hat{u}_s - \hat{v}_s, \hat{\psi}^u)_{\widehat{\Omega}_s} \quad = 0 \quad \forall\hat{\psi}^u \in \hat{L}_s,\right.$$

$$\left\{(\widehat{div}(\hat{J}\widehat{F}^{-1}\hat{v}_f), \hat{\psi}^p)_{\widehat{\Omega}_f} \quad = 0 \quad \forall\hat{\psi}^p \in \hat{L}_f^0.\right.$$

The stress tensors for fluid, solid and mesh motion read:

$$\widehat{\sigma}_f = -\hat{p}_f \hat{I} + 2\hat{\rho}_f \nu_f (\widehat{\nabla} \hat{v}_f \widehat{F}^{-1} + \widehat{F}^{-T} \widehat{\nabla} \hat{v}_f^T),$$
$$\widehat{\Sigma} = 2\mu_s \widehat{E} + \lambda_s tr\widehat{E}\hat{I}, \quad \text{with the strain } \widehat{E} = \frac{1}{2}(\widehat{F}^T \widehat{F} - \hat{I}),$$
$$\widehat{\sigma}_{mesh} = \hat{J}^{-1} \alpha_u \widehat{\nabla} \hat{u}_f,$$

with the densities $\hat{\rho}_f$ and $\hat{\rho}_s$, fluid's viscosity ν_f. The solid parameters are given by the Lamé parameters μ_s, λ_s and the normal vector is $\hat{n}_f$. Finally, $\hat{J}^{-1}\alpha_u > 0$ is used to control the fluid mesh motion.

2.2 Variational phase-field for dynamic pressurized-fractures

In phase-field-based fracture propagation, the unknown solution variables are displacements $u : \Omega_s \cup \overline{\mathcal{C}} \to \mathbb{R}^2$ and a smoothed indicator phase-field function $\varphi : \Omega_s \cup \overline{\mathcal{C}} \to [0,1]$. Here $\varphi = 0$ denotes the crack region and $\varphi = 1$ characterizes the unbroken material. The intermediate values constitute a smooth transition zone dependent on a regularization parameter ε. The physics of the underlying problem ask to enforce a crack irreversibility condition (the crack can never heal) that is an inequality condition in time: $\partial_t \varphi \leq 0$. Consequently, modeling of fracture evolution problems leads to a variational inequality system, that is, due to this constraint, quasi-stationary or time-dependent. Our system of equations applies to cracks in elasticity and pressurized fractures. In the latter one, a nonhomogeneous Neumann condition is applied to the crack surface; a detailed derivation and corresponding mathematical analysis can be found in [17,16]. The resulting Euler-Lagrange system, while additionally including the solid acceleration term, then reads:

Proposition 3. *Let $p_F \in H^1(\Omega_s \cup \mathcal{C})$ and $\tilde{\varphi}$ (see [9]) be given. Find $(u, \varphi) \in \{u_D + H_0^1(\Omega_s \cup \mathcal{C})\} \times W$ for almost all times $t \in (0, T]$ such that*

$$\Big\{ (\rho_s \partial_t^2 u, \psi^u) + \Big(\big((1-\kappa)\tilde{\varphi}^2 + \kappa\big)\, \Sigma(u), \nabla \psi^u \Big) + (\tilde{\varphi}^2 p_F, \nabla \cdot \psi^u) = 0 \;\forall \psi^u \in V,$$
$$\begin{cases} (1-\kappa)(\varphi\, \Sigma(u) : e(u), \psi^\varphi - \varphi) + 2(\varphi\, p_F\, \nabla \cdot u, \psi^\varphi - \varphi) \\ + G_c \Big(-\frac{1}{\varepsilon}(1-\varphi, \psi^\varphi - \varphi) + \varepsilon(\nabla\varphi, \nabla(\psi^\varphi - \varphi)) \Big) \geq 0 \;\forall \psi^\varphi \in W \cap L^\infty(\Omega_s \cup \mathcal{C}). \end{cases}$$

In Proposition 3, κ is a positive regularization parameter for the elastic energy, with $\kappa = o(\varepsilon)$, and G_c is the critical energy release rate. Furthermore, Σ is the linearized version of $\widehat{\Sigma}$ with $E = \frac{1}{2}(\nabla u + \nabla u^T)$.

2.3 The final system

We collect all pieces and perform two additional steps in Proposition 3:

- transforming from $\Omega_s \cup \mathcal{C}$ to $\widehat{\Omega}_s \cup \widehat{\mathcal{C}}$ and re-defining the space W in terms of $\hat{W}$, respectively;

– introducing the augmented Lagrangian penalization strategy to treat the variational inequality.

We then obtain

Proposition 4. *Let $p_F \in H^1(\widehat{\Omega}_s \cup \widehat{\mathcal{C}})$ be given. Find vector-valued velocities, vector-valued displacements, a scalar-valued fluid pressure, and a scalar-valued phase-field function, that is to say that $\{\hat{v}_f, \hat{v}_s, \hat{u}_f, \hat{u}_s, \hat{p}_f, \hat{\varphi}_s\} \in \{\hat{v}_f^D + \hat{V}_{f,\hat{v}}^0\} \times \hat{L}_s \times \{\hat{u}_f^D + \hat{V}_{f,\hat{u}}^0\} \times \{\hat{u}_s^D + \hat{V}_s^0\} \times \hat{L}_f^0 \times H^1(\widehat{\Omega}_s \cup \widehat{\mathcal{C}})$, such that $\hat{v}_f(0) = \hat{v}_f^0$, $\hat{v}_s(0) = \hat{v}_s^0$, $\hat{u}_f(0) = \hat{u}_f^0$, $\hat{u}_s(0) = \hat{u}_s^0$ and $\hat{\varphi}_s(0) = \hat{\varphi}_s^0$ are satisfied, and for almost all times $t \in (0, T]$ holds:*

$$\textit{Fluid momentum} \begin{cases} (\hat{J}\hat{\rho}_f \partial_t \hat{v}_f, \hat{\psi}^v)_{\widehat{\Omega}_f} + (\hat{\rho}_f \hat{J}(\widehat{F}^{-1}(\hat{v}_f - \hat{w}) \cdot \widehat{\nabla})\hat{v}_f), \hat{\psi}^v)_{\widehat{\Omega}_f} \\ +(\hat{J}\hat{\sigma}_f \widehat{F}^{-T}, \widehat{\nabla}\hat{\psi}^v)_{\widehat{\Omega}_f} \\ +\langle \rho_f \nu_f \hat{J}(\widehat{F}^{-T}\widehat{\nabla}\hat{v}_f^T \hat{n}_f)\widehat{F}^{-T}, \hat{\psi}^v \rangle_{\widehat{\Gamma}_{out}} = 0 \quad \forall \hat{\psi}^v \in \hat{V}_{f,\widehat{\Gamma}_i}^0, \end{cases}$$

$$\textit{Solid momentum, 1st eq.} \begin{cases} (\hat{\rho}_s \partial_t \hat{v}_s, \hat{\psi}^v)_{\widehat{\Omega}_s} + \Big(\big((1-\kappa)\tilde{\varphi}^2 + \kappa\big)\widehat{F}\widehat{\Sigma}, \widehat{\nabla}\hat{\psi}^v \Big)_{\widehat{\Omega}_s} \\ +(\tilde{\varphi}^2 p_F, \widehat{\nabla} \cdot \hat{\psi}^v) \quad = 0 \quad \forall \hat{\psi}^v \in \hat{V}_s^0, \end{cases}$$

$$\textit{Fluid mesh motion} \Big\{ (\widehat{\sigma}_{mesh}, \widehat{\nabla}\hat{\psi}^u)_{\widehat{\Omega}_f} \quad = 0 \quad \forall \hat{\psi}^u \in \hat{V}_{f,\hat{u},\widehat{\Gamma}_i}^0,$$

$$\textit{Solid momentum, 2nd eq.} \Big\{ \hat{\rho}_s(\partial_t \hat{u}_s - \hat{v}_s, \hat{\psi}^u)_{\widehat{\Omega}_s} \quad = 0 \quad \forall \hat{\psi}^u \in \hat{L}_s,$$

$$\textit{Fluid mass conservation} \Big\{ (\widehat{div}(\hat{J}\widehat{F}^{-1}\hat{v}_f), \hat{\psi}^p)_{\widehat{\Omega}_f} \quad = 0 \quad \forall \hat{\psi}^p \in \hat{L}_f^0.$$

$$\textit{Phase-field} \begin{cases} (1-\kappa)(\hat{J}\hat{\varphi}_s\, \widehat{\Sigma} : \widehat{E}, \hat{\psi}^\varphi)_{\widehat{\Omega}_s} + 2(\hat{J}\hat{\varphi}_s\, p_F\, \widehat{\nabla} \cdot \hat{u}_s, \hat{\psi}^\varphi)_{\widehat{\Omega}_s} \\ +G_c \Big(-\frac{1}{\varepsilon}(\hat{J}(1-\hat{\varphi}_s), \hat{\psi}^\varphi) + \varepsilon(\hat{J}(\widehat{\nabla}\hat{\varphi}_s \widehat{F}^{-1})\widehat{F}^{-T}, \widehat{\nabla}\hat{\psi}^\varphi) \Big)_{\widehat{\Omega}_s} \\ +\big(\hat{J}[\Xi + \gamma \partial_t \hat{\varphi}_s]^+, \hat{\psi}^\varphi\big)_{\widehat{\Omega}_s} \quad = 0 \quad \forall \hat{\psi}^\varphi \in H^1(\widehat{\Omega}_s \cup \widehat{\mathcal{C}}). \end{cases}$$

Remark 5. The continuous penalization constraint $[\Xi + \gamma \partial_t \hat{\varphi}_s]^+$ with $\Xi \in L^2$ and $\gamma > 0$ and $[x]^+ = \max(0, x)$ is numerically realized based on the incremental formulation as explained in [19].

Remark 6. The system in Proposition 4 has been implemented as presented. However the numerical example below deals with moderate deformations; namely $\|\widehat{\nabla}\hat{u}\| \ll 1$ and thus $\widehat{F} \approx \hat{I}$ and $\hat{J} \approx 1$ such that the phase-field fracture model can be classified as proposed in [8,14] and where linear elastic fracture mechanics applies. Testing large FSI-solid deformations, including fractures, is subject of ongoing studies.

Remark 7. We emphasize that the given p_F in the pressurized phase-field fracture framework is neither coupled to the Navier-Stokes pressure $\hat{p}_f$ nor do we allow that the fracture reaches the FSI interface $\widehat{\Gamma}_i$. Mathematical modeling of these processes has not yet been established. Preliminary work into this direction where a quasi-static fluid-filled phase-field fracture is coupled to flow in a porous medium has been recently undertaken in [15,17].

3 Aspects of Discretization and the Solution Algorithm

The coupled FSI phase-field problem in Proposition 4 is first formulated in terms of single semilinear form and then solved with the Rothe method: first time, then space. Specifically, time discretization is based on a One-step-θ scheme (here $\theta = 0.5 + \delta$, where $\delta = 0.01$ is related to the time step size $k = t^{n+1} - t^n$; resulting in A-stable (second order) stabilized Crank-Nicolson time-stepping) as presented for the pure FSI problem, Proposition 2, in [20]. Computational stability of these schemes has been investigated in [18]. In space, the problem is discretized with conforming finite elements on a quadrilateral mesh. For the fluid, an inf-sup stable velocity-pressure pair is chosen, Q_2^c/P_1^{dc}; for the displacements Q_2^c and for the phase-field variable Q_1^c. The fully-coupled nonlinear problem is solved with Newton's method as explained for pure FSI in detail in [20]. In particular, the Jacobian is constructed from the analytical evaluation of the directional derivatives. As linear solver we use UMFPACK [6], which is motivated by the fact that the numerical example is 2D and that preconditioners for the fully-coupled system are extremely difficult to be developed and out of scope in this contribution.

4 A Prototype Numerical Example

The example is computed with the finite element package deal.II [1] by implementing the method from [19] in the open source FSI code related to [20].

Configuration Details on the geometry can be found in Figure 1. Here, the initial fracture is initialized by the initial condition $\hat{\varphi}^0 = 0$ in $(0.875, 0.9375) \times (0.25, 0.625)$. Three mesh levels are obtained from uniform refinement resulting in $2\,048, 8\,192$ and $32\,768$ mesh cells. For the upper, lower, and left boundaries, the 'no-slip' conditions for velocity and no zero displacement for the solid are given. At the fluid outlet $\hat{\Gamma}_{out}$, the 'do-nothing' outflow condition [10] is imposed. A parabolic inflow velocity profile is given on $\hat{\Gamma}_{in}$ by

$$v_f(0, y) = \bar{U}(y - 1)(y - 0.5), \quad \bar{U} = 1.0ms^{-1}.$$

For $t < 2.0s$, $v_f(0, y)$ is scaled with $\frac{1-\cos(\frac{\pi}{2}t)}{2}$ in order to have a smooth inflow profile.

Parameters For the fluid we use $\varrho_f = 1kgm^{-3}$, $\nu_f = 10^{-2}m^2s^{-1}$ resulting in stationary flow. The elastic solid is characterized by $\varrho_s = 10kgm^{-3}$, $\nu_s = 0.2$, $\mu_s = 1kgm^{-1}s^{-2}$. The fracture pressure is $p_F = 10^{-2}Pa$. The model parameter $\varepsilon = 0.044 = h_{coarse}$ is fixed in all computations as well as $\kappa = 10^{-10}$. Furthermore, $\gamma = 50$ and $G_c = 1N/m$. The (absolute) Newton tolerance is chosen as 10^{-10}. Three augmented Lagrangian steps are performed per time step. The time step size is $k = 1s$ and the total time $T = 10s$.

Quantities of interest We evaluate $\hat{u}_x(1, 0.75)$, the normal stress in x-direction (i.e., drag) along the FSI-interface, and a line integral, i.e., COD $= \int_{\{0 \le x \le 2; y = 0.4375\}} \hat{u}\widehat{\nabla}\hat{\varphi}\, d\hat{s}$. Here, COD is related to the crack opening displacement in pure fracture problems. In addition, we check $\min(\hat{J}) > 0$.

Discussion of our findings Our results are provided in Figure 2 and Table 1.

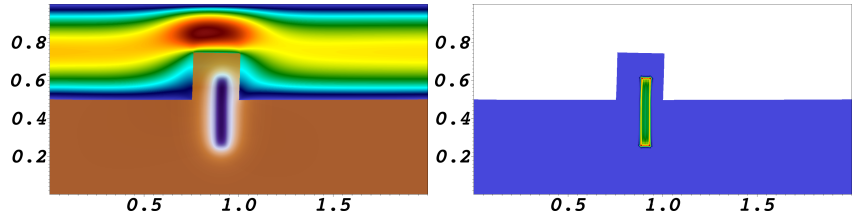

Fig. 2. At left: velocity field including the fracture pattern (in blue) in the brown solid zone. On the right, the penalty function Ξ is shown. The penalty is specifically active at the fracture boundary and the four corners (red). In the blue and white zones, we have $\Xi = 0$.

Table 1. Goal functional evaluations on three different meshes at $T = 10s$.

Cells	DoFs	$h[m]$	$\hat{u}_x[\times 10^{-2}m]$	Drag$[\times 10^{-3}N]$	COD$[\times 10^{-4}m]$	$\min(\hat{J})$
2048	41829	0.044	1.851	2.995	-03.339	0.787
8192	165573	0.022	1.979	2.858	-11.447	0.717
32768	658821	0.011	2.077	2.771	-15.293	0.621

5 Conclusions

In this work, fluid-structure interaction has been coupled with a phase-field model for pressurized-fractures. The proposed framework is formulated in a variational-monolithic setting that ensures high accuracy of the coupling conditions. The emphasize in this work was on the model statement and a prototype numerical example. Therefore, the phase-field methodology has been rather used to represent a stationary pressurized fracture but not yet a propagating crack. Current work is based on adapting the different flow, solid, and fracture parameters to carry out fully nonstationary fluid-structure interaction with given and propagating fractures.

References

1. W. Bangerth, T. Heister, and G. Kanschat, *Differential equations analysis library*, 2012.
2. M. J. Borden, C. V. Verhoosel, M. A. Scott, T. J. R. Hughes, and C. M. Landis, *A phase-field description of dynamic brittle fracture*, Comput. Meth. Appl. Mech. Engrg. **217** (2012), 77–95.
3. B. Bourdin, *Numerical implementation of the variational formulation for quasi-static brittle fracture*, Interfaces and free boundaries **9** (2007), 411–430.
4. B. Bourdin, G. Francfort, and J.-J. Marigo, *The variational approach to fracture*, J. Elasticity **91**:1–3 (2008), 1–148.
5. B. Bourdin, C. Larsen, and C. Richardson, *A time-discrete model for dynamic fracture based on crack regularization*, Int. J. Frac. **168**:2 (2011), 133–143.

6. T. A. Davis and I. S. Duff, *An unsymmetric-pattern multifrontal method for sparse LU factorization*, SIAM J. Matrix Anal. Appl. **18**:1 (1997), 140–158.
7. J. Donea, S. Giuliani, and J. Halleux, *An arbitrary lagrangian-eulerian finite element method for transient dynamic fluid-structure interactions*, Comput. Methods Appl. Mech. Engrg. **33** (1982), 689–723.
8. G. Francfort and J.-J. Marigo, *Revisiting brittle fracture as an energy minimization problem*, J. Mech. Phys. Solids **46**:8 (1998), 1319–1342.
9. T. Heister, M. F. Wheeler, and T. Wick, *A primal-dual active set method and predictor-corrector mesh adaptivity for computing fracture propagation using a phase-field approach*, Comp. Meth. Appl. Mech. Engrg. **290**:0 (2015), 466 – 495.
10. J. G. Heywood, R. Rannacher, and S. Turek, *Artificial boundaries and flux and pressure conditions for the incompressible Navier-Stokes equations*, International Journal of Numerical Methods in Fluids **22** (1996), 325–352.
11. J. Hron and S. Turek, A monolithic FEM/Multigrid solver for ALE formulation of fluid structure with application in biomechanics, vol. 53, 146–170, Springer-Verlag, 2006, pp. 146–170.
12. T. Hughes, W. Liu, and T. Zimmermann, *Lagrangian-Eulerian finite element formulation for incompressible viscous flows*, Comput. Methods Appl. Mech. Engrg. **29** (1981), 329–349.
13. C. J. Larsen, C. Ortner, and E. Süli, *Existence of solutions to a regularized model of dynamics fracture*, Methods in Applied Sciences **20** (2010), 1021–1048.
14. C. Miehe, F. Welschinger, and M. Hofacker, *Thermodynamically consistent phase-field models of fracture: variational principles and multi-field fe implementations*, Int. J. Numer. Methods Engrg. **83** (2010), 1273–1311.
15. A. Mikelić, M. F. Wheeler, and T. Wick, *A phase-field method for propagating fluid-filled fractures coupled to a surrounding porous medium*, SIAM Multiscale Model. Simul. **13**:1 (2015), 367–398.
16. ———, *A quasi-static phase-field approach to pressurized fractures*, Nonlinearity **28**:5 (2015), 1371–1399.
17. A. Mikelić, M. Wheeler, and T. Wick, *Phase-field modeling of a fluid-driven fracture in a poroelastic medium*, accepted in Computational Geosciences, doi: 10.1007/s10596-015-9532-5, Sep 2013.
18. T. Richter and T. Wick, *On time discretizations of fluid-structure interactions*, Multiple Shooting and Time Domain Decomposition Methods (T. Carraro, M. Geiger, S. Körkel, and R. Rannacher, eds.), Contributions in Mathematical and Computational Science, 2015.
19. M. Wheeler, T. Wick, and W. Wollner, *An augmented-Lagangrian method for the phase-field approach for pressurized fractures*, Comp. Meth. Appl. Mech. Engrg. **271** (2014), 69–85.
20. T. Wick, *Fluid-structure interactions using different mesh motion techniques*, Computers and Structures **89**:13-14 (2011), 1456–1467.